Trends in Global Tropical Cyclone Activity: 1990-2020

Klotzbach Philip[1], Wood Kimberly M.[2], Schreck Carl[3], Bowen Steven G.[4], Patricola Christina M[5], and Bell Michael[1]

[1]Colorado State University
[2]Mississippi State University
[3]North Carolina State University
[4]Aon
[5]Iowa State University

November 16, 2022

Abstract

This study investigates trends in global tropical cyclone (TC) activity from 1990–2020, a period where observational platforms are mostly consistent. Several global TC metrics have decreased during this period, with significant decreases in hurricanes and Accumulated Cyclone Energy (ACE). Most of this decrease has been driven by significant downward trends in the western North Pacific. Globally, short-lived named storms, 24-hr intensification periods of >=50 kt day^{-1} and TC-related damage have increased significantly. The increase in short-lived named storms is likely due to technological improvements, while rapidly intensifying TC increases may be fueled by higher potential intensity. Damage increases are largely due to increased coastal assets. The decreasing trends in hurricane numbers and global ACE are likely due to the trend towards a more La Niña-like base state from 1990–2020, favoring TC activity in the North Atlantic and suppressing TC activity in the eastern and western North Pacific.

Trends in Global Tropical Cyclone Activity: 1990–2020

P. J. Klotzbach[1], K. M. Wood[2*], C. J. Schreck[3], S. G. Bowen[4], C. M. Patricola[5], and M. M. Bell[1]

[1]Department of Atmospheric Science, Colorado State University, Fort Collins, CO, USA.

[2]Department of Geosciences, Mississippi State University, Mississippi State, MS, USA.

[3]Cooperative Institute for Satellite Earth System Studies (CISESS), North Carolina State University, Asheville, NC, USA.

[4]Aon, Chicago, IL, USA.

[5]Department of Geological and Atmospheric Sciences, Iowa State University, Ames, IA, USA.

*Klotzbach and Wood contributed equally to this work

Corresponding author: Philip Klotzbach (philk@atmos.colostate.edu)

Key Points:

- Global hurricane counts and Accumulated Cyclone Energy have significantly trended downward since 1990 due to a trend towards La Niña.
- Short-lived named storms, extreme RI periods (50+ kt day^{-1}) and global damage have increased significantly from 1990–2020.
- Decreasing trend in global hurricanes and Accumulated Cyclone Energy is primarily driven by downturn in western North Pacific activity.

Abstract

This study investigates trends in global tropical cyclone (TC) activity from 1990–2020, a period where observational platforms are mostly consistent. Several global TC metrics have decreased during this period, with significant decreases in hurricanes and Accumulated Cyclone Energy (ACE). Most of this decrease has been driven by significant downward trends in the western North Pacific. Globally, short-lived named storms, 24-hr intensification periods of >=50 kt day^{-1} and TC-related damage have increased significantly. The increase in short-lived named storms is likely due to technological improvements, while rapidly intensifying TC increases may be fueled by higher potential intensity. Damage increases are largely due to increased coastal assets. The decreasing trends in hurricane numbers and global ACE are likely due to the trend towards a more La Niña-like base state from 1990–2020, favoring TC activity in the North Atlantic and suppressing TC activity in the eastern and western North Pacific.

Plain Language Summary

This study investigates trends in global tropical cyclone activity from 1990–2020 - a period characterized by consistent satellite observing platforms. We find a significant decreasing trend in global hurricanes and Accumulated Cyclone Energy – an integrated metric accounting for hurricane frequency, intensity and duration. This decreasing trend has primarily been driven by a significant decreasing trend in the western North Pacific – the climatologically most active global tropical cyclone basin. Short-lived named storms (tropical cyclones lasting <=2 days) and 24-hr periods where storms have intensified by >=50 kt day^{-1} have increased significantly since 1990. Also, global damage from TCs has significantly increased. The increase in short-lived named storms is likely due to improved sensors, while the increase in rapidly intensifying storms may be driven by more favorable thermodynamics. Damage increases are largely due to growth in population and increased value of assets (physical structures and non-physical risk exposure) along the coast. The trend during the past 31 years towards a more La Niña-like environment has favored tropical cyclone activity over the North Atlantic and suppressed activity over the North Pacific. Since the North Pacific generates much more activity than the Atlantic climatologically, global tropical cyclone activity has generally trended downward.

1 Introduction

Tropical cyclones (TCs) are one of the most damaging global natural catastrophes, causing hundreds of fatalities and billions of US dollars in damage each year (Mendelsohn et al., 2012; Klotzbach et al., 2018). Consequently, scientists have extensively explored the potential impacts of human-induced climate change on TC frequency, intensity, and associated metrics that have been recently summarized by Knutson et al. (2019, 2020). These studies examined observed trends in these TC metrics (Knutson et al., 2019) as well as projections of future TC activity using various climate models (Knutson et al., 2020). While future projections of TC activity are an important area of research, this manuscript focuses on recent observed trends in TC activity.

Several studies over the past two decades have examined trends in global TC activity, with Webster et al. (2005) noting a near-doubling of global Category 4–5 hurricanes on the Saffir-Simpson Hurricane Wind Scale (SSHWS; maximum 1-minute sustained winds >=113 kt) from 1970–2004. However, subsequent studies argued that changes to the observational network (e.g., improved satellite capability) in the 1970s and 1980s likely contributed to those large observed increases (Landsea et al., 2006). During 1986–2005, Klotzbach (2006) noted only a small insignificant increasing trend (~10%) in Category 4–5 hurricanes and an insignificant decreasing trend in global Accumulated Cyclone Energy (ACE; Bell et al. 2000) – an integrated metric that accounts for frequency, intensity, and duration of TCs. Klotzbach and Landsea (2015) updated the results of Webster et al. (2005) using ten additional years of data (e.g., 1970–2014) and found that between 1990 and 2014, there was a slight insignificant downward trend in Category 4–5 hurricane frequency and a slight insignificant upward trend in the percentage of hurricanes reaching Category 4–5 intensity. Consequently, they argued that most of the increase noted by Webster et al. (2005) was due to changes in observational platforms, primarily in the 1970s and 1980s. Recently, Kossin et al. (2020) found a significant increasing trend in the ratio of major (Category 3+ on the SSHWS; >=96 kt) hurricane observations to all hurricane observations using ADT-HURSAT, a satellite-derived TC intensity dataset, from 1979–2017.

Maue (2011) found that neither global ACE nor named storm frequency showed a significant long-term trend during 1970–2011, with global ACE in 2010/11 at its lowest levels since the late 1970s. He attributed the downturn in ACE to the transition of the Pacific decadal oscillation (PDO; Mantua & Hare, 2002) to its negative phase and several strong La Niña events that tend to suppress ACE in the climatologically active Pacific.

In addition to global TC frequency and intensity metrics, other studies have examined trends in TC rapid intensification (RI). Though various RI thresholds have been used, the canonical definition involves an increase in TC intensity by 30+ kt day^{-1}, representing approximately the 95th percentile of 24-hr over-water TC intensification rates in the North Atlantic (Kaplan & DeMaria, 2003). Balaguru et al. (2018) found a significant increasing trend of the 95th percentile of 24-hr intensity changes in the eastern and central tropical Atlantic from 1986–2015. Bhatia et al. (2019) examined both observational data from the National Hurricane Center (NHC) and Joint Typhoon Warning Center (JTWC) (the same as used in this manuscript) as well as ADT-HURSAT from 1982–2009 and found significant increasing trends for global TCs as well as North Atlantic TCs specifically at the highest intensity change quantiles in both datasets.

Several studies have examined trends in TC-related damage and highlighted increases for both the United States (Klotzbach et al., 2018; Weinkle et al., 2018; Grinsted et al., 2019) and for the globe (Weinkle et al., 2012). These increases have been largely attributed to growth in population and the increased value of coastal assets (physical structures and non-physical risk exposure), but increases in TC intensity may also play a role (Grinsted et al., 2019).

Prior to 1990, data issues likely preclude an accurate estimate of global TC intensities. No direct geostationary satellite data over the North and South Indian Oceans were available until *Meteosat-5* was launched in 1989 (Knapp and Kossin, 2007). Also, the transfer of responsibility for the eastern North Pacific from the Weather Service Forecast Office, Redwood City, California, to the National Hurricane Center following the 1987 hurricane season may have led to a jump in analyzed intensities (Klotzbach and Landsea, 2015). Consequently, this study examines trends in the above-discussed TC metrics and other related metrics using observational data from 1990–2020 (Landsea et al., 2006; Klotzbach and Landsea, 2015). We also examine large-scale atmospheric and oceanic patterns that may be responsible for the observed trends.

2 Data and Methodology

Global TC data from 1990–2019 are obtained from US warning agency best tracks: the National Hurricane Center/Central Pacific Hurricane Center best track (e.g., HURDAT2; Landsea and Franklin, 2013) for the North Atlantic and eastern North Pacific basins and the Joint Typhoon Warning Center best track (Chu et al., 2002) for all remaining TC basins as hosted by the International Best Track Archive for Climate Stewardship version 4 (IBTrACSv4; Knapp et al., 2010). Operational best track data as archived in IBTrACSv4 is used for the 2020 TC season.

We define TC basins following Knapp et al. (2010) and Klotzbach and Landsea (2015), dividing the eastern North Pacific and western North Pacific basins at the International Date Line and the South Indian and South Pacific basins at 135°E. While noting that Southern Hemisphere TC seasons are typically defined to cover 1 July to 30 June, in this study, we examine trends in calendar year TC activity. A storm is counted based on the year that it reached a particular threshold, so if a TC reached tropical storm intensity on 30 December and hurricane intensity on 2 January, it would count as a named storm in the first year and a hurricane in the second year. If a TC extends from one calendar year to the next, it is only counted in the calendar year where it formed. Though various names are used for TCs depending on TC basin (e.g., typhoon, cyclone), we use the term "hurricane" to collectively refer to all TCs reaching hurricane strength (>=64 kt) regardless of the ocean basin where they developed.

We calculate 24-hr RI events and evaluate them at two thresholds: 30 kt and 50 kt. If a TC intensified by a specific threshold for adjacent 24-hr periods, it would count as multiple RI events. Given uncertainties in tropical depression intensity estimates (e.g., Klotzbach & Landsea, 2015), we only calculate RI events for TCs that were at least tropical-storm strength (e.g., >=34 kt) at the beginning of their RI episode. We also evaluate over-ocean rapid weakening (RW; Wood & Ritchie, 2015) events at thresholds of -30 kt and -50 kt in 24 hr. To be included as RW events, the TC center must remain >= 100 km from land and the TC intensity >= 34 kt throughout the 24-hr period.

The ENSO Longitude Index (ELI; Williams & Patricola, 2018) estimates the average longitude of deep convection associated with the Walker Circulation and is consequently preferred to classify the ENSO state over the canonical Nino 3.4 index (Barnston et al., 1997) due to its improved ability to capture various ENSO spatial characteristics. ELI is calculated using monthly SST from the Extended Reconstructed Sea Surface Temperature (ERSSTv5) dataset (Huang et al., 2017).

Global damage is obtained from EM-DAT (EM-DAT, 2021) with additional damage as archived by Aon in public annual catastrophe reports and their proprietary Catastrophe Insight Database.

The fifth-generation reanalysis from the European Centre for Medium Range Weather Forecasts (ERA5; Hersbach et al. 2019) is utilized for all atmospheric and oceanic calculations in this manuscript. The ERA5 is produced at a 0.25° spatial resolution and a one-hourly temporal resolution. Here we use ERA5 data at a monthly temporal resolution.

Statistical significance of least-squares linear trends are calculated using a two-tailed Student's t-test and treating each year as an individual degree of freedom given the low autocorrelation between one year's global TC activity and the next year's global TC activity. For environmental fields, significance of trends is calculated using a two-tailed Wald test via *SciPy*. Statistical significance is reported at 5% and 10% levels throughout the manuscript.

3 Trends in Tropical Cyclone Activity

Figure 1 highlights trends for several global TC activity metrics from 1990–2020. Table S1 provides average global TC activity for these and additional calculated metrics and the percentage contribution of each basin to the global total. Table S2 states the numerical values of linear trends for each index in Figure 1 as well as several additional indices. Category 4–5 percentage trends in Figure 1 and Table S2 are displayed in percentage increase/decrease per decade; that is, if a basin's Category 4–5 percentage increased from 36% to 42% over the 31-year period, it would be displayed as a ~2% increase per decade. Category 4–5 hurricane percentage linear trends are not displayed for the North Indian Ocean due to limited per-year hurricane formations.

The western North Pacific generates the most TC activity for each parameter investigated, producing a higher percentage of the global total for more intense metrics (e.g., Category 4–5 hurricanes vs. named storms; see Table S1). While only accounting for 11% of global Category 4–5 hurricanes and 15% of global ACE, TCs in the North Atlantic basin caused 62% of global damage.

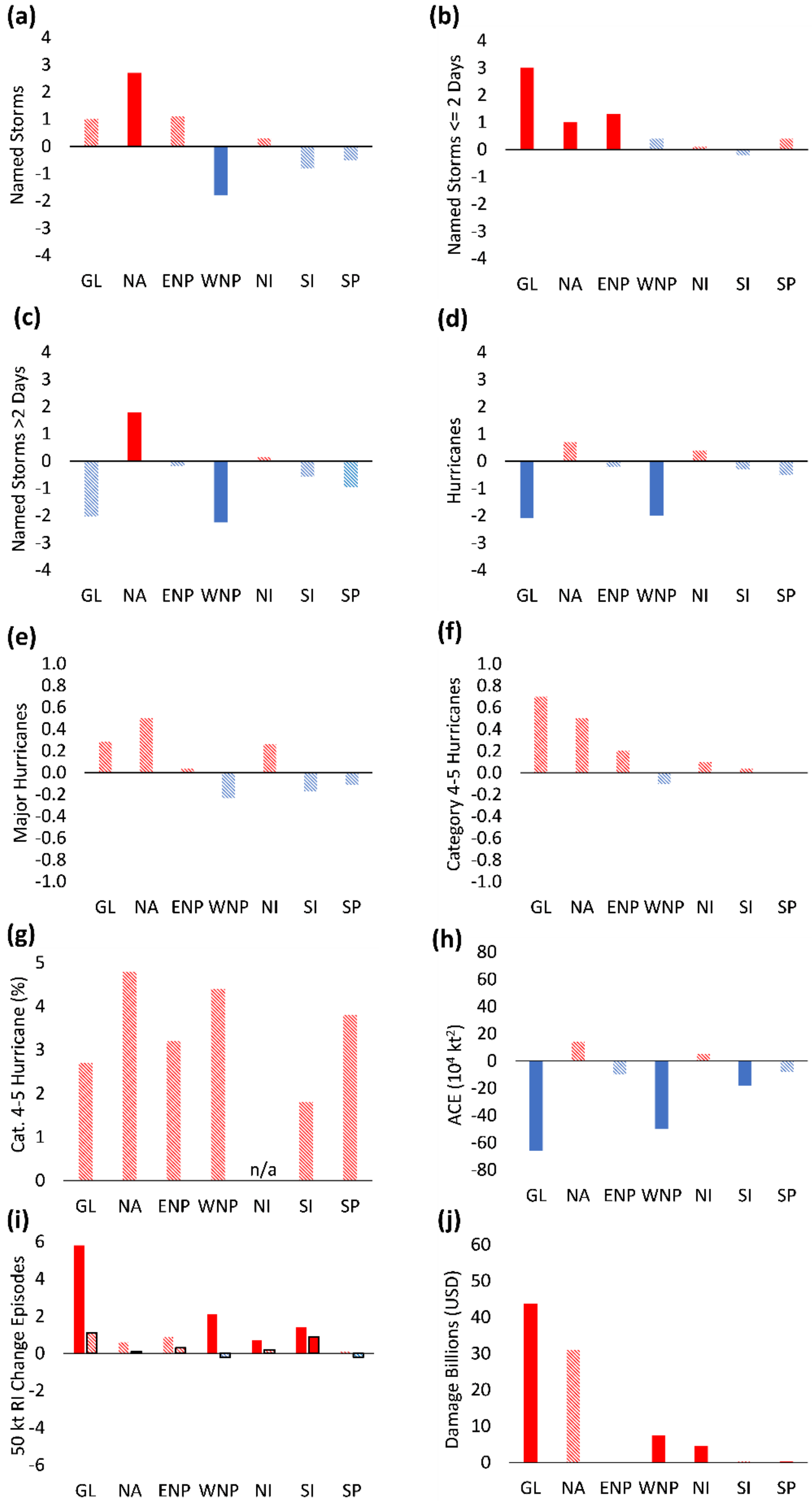
(a)
Named Storms
4
3
2
1
0
-1
-2
-3
-4
GL NA ENP WNP NI SI SP
(b)
Named Storms <= 2 Days
4
3
2
1
0
-1
-2
-3
-4
GL NA ENP WNP NI SI SP
(c)
Named Storms >2 Days
4
3
2
1
0
-1
-2
-3
-4
GL NA ENP WNP NI SI SP
(d)
Hurricanes
4
3
2
1
0
-1
-2
-3
-4
GL NA ENP WNP NI SI SP
(e)
Major Hurricanes
1.0
0.8
0.6
0.4
0.2
0.0
-0.2
-0.4
-0.6
-0.8
-1.0
GL NA ENP WNP NI SI SP
(f)
Category 4-5 Hurricanes
1.0
0.8
0.6
0.4
0.2
0.0
-0.2
-0.4
-0.6
-0.8
-1.0
GL NA ENP WNP NI SI SP
(g)
Cat. 4-5 Hurricane (%)
5
4
3
2
1
0
n/a
GL NA ENP WNP NI SI SP
(h)
ACE (10^4 kt^2)
80
60
40
20
0
-20
-40
-60
-80
GL NA ENP WNP NI SI SP
(i)
50 kt RI Change Episodes
6
4
2
0
-2
-4
-6
GL NA ENP WNP NI SI SP
(j)
Damage Billions (USD)
60
50
40
30
20
10
0
GL NA ENP WNP NI SI SP

Figure 1. Per-decade linear trends for (a) named storms, (b) named storms lasting <= 2 days, (c) named storms lasting >2 days, (d) hurricanes, (e) major hurricanes, (f) Category 4–5 hurricanes, (g) Category 4–5 hurricane percentage, (h) ACE, (i) 50-kt RI and RW episodes (highlighted with black borders) and (j) damage (in billions USD). Trends significant at the 10% level are displayed with solid bars, and insignificant trends are lighter in color and hashed.

Figure 2a displays global named storms (e.g., TCs with maximum sustained winds >=34 kt) by calendar year from 1990–2020. There is a weak, insignificant upward trend in global named storm activity during the 31-year period, with a significant increasing trend in North Atlantic TC activity and a significant decreasing trend in western North Pacific TC activity (Fig. 1a).

Figure 2b focuses on TCs of named storm strength for <= 2 days. Landsea et al. (2010) noted a significant increase in these short-lived named storms in the North Atlantic that occurred around 2000 associated with improved microwave sensors, scatterometry, and use of the cyclone phase space diagram (Hart, 2003). Both the North Atlantic and eastern North Pacific basins have shown significant increases in short-lived named storms over the 31-year period (Fig. 1b), likely due to improved technology. Other basins show insignificant trends in short-lived named storms.

Figure 2c shows named storms lasting >2 days, likely a more robust metric of longer-term variability in global named storm activity. Globally, named storms have decreased by 2 storms per decade, although this decreasing trend is insignificant (Fig. 1c). While not significant, a decrease in global named storm activity is generally expected by most climate models with continued anthropogenic climate change (Knutson et al., 2020b). Throughout the 31-year period, named storms lasting >2 days have significantly increased in the North Atlantic and significantly decreased in the western North Pacific (Fig. 1c).

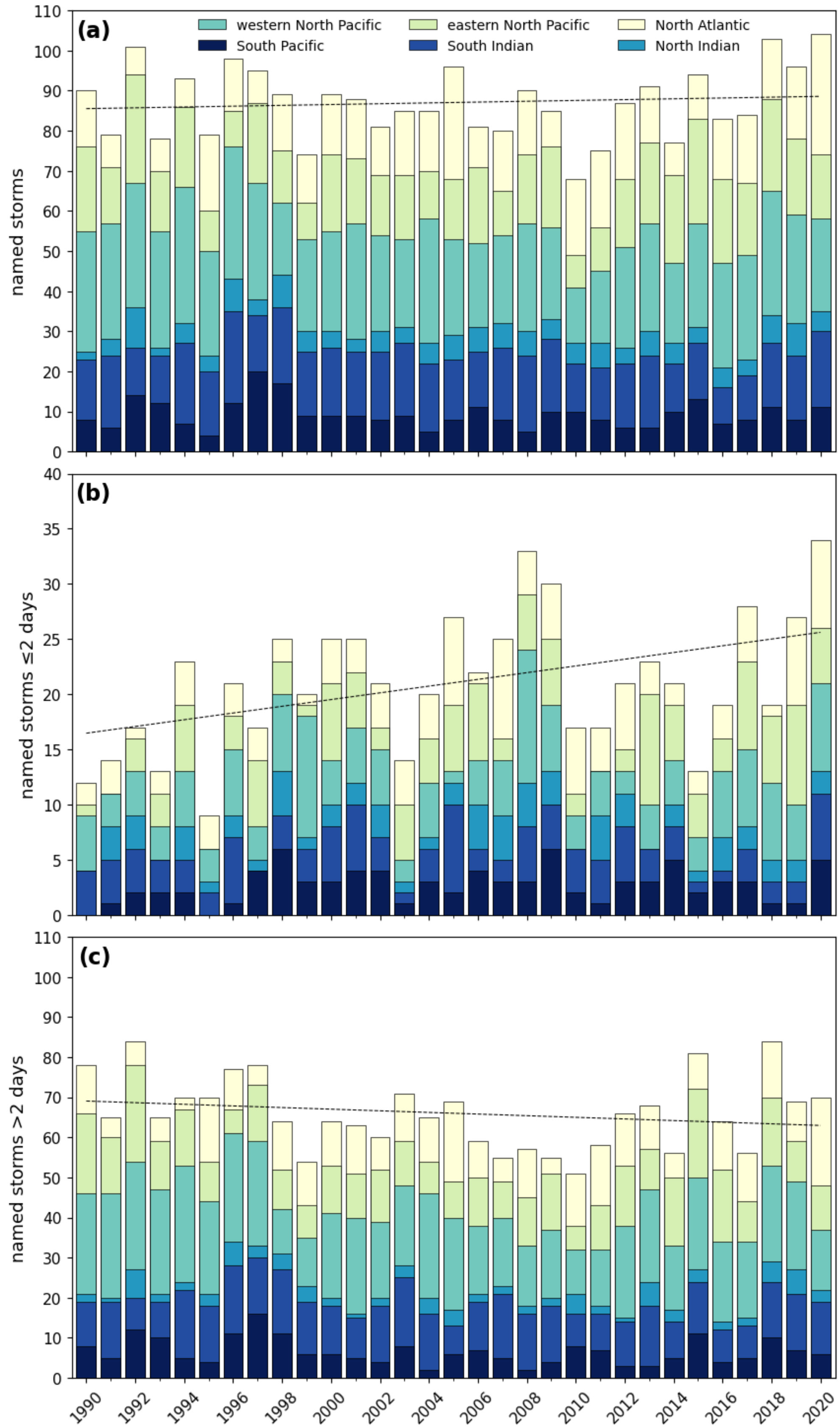
(a)
western North Pacific
eastern North Pacific
North Atlantic
South Pacific
South Indian
North Indian
named storms
(b)
named storms ≤2 days
(c)
named storms >2 days
1990
1992
1994
1996
1998
2000
2002
2004
2006
2008
2010
2012
2014
2016
2018
2020

Figure 2. Global named storm formations during 1990–2020. (a) Named storm formations in six TC basins: western North Pacific, eastern North Pacific, North Atlantic, North Indian, South Indian, and South Pacific. (b) As in (a) but for named storms lasting <=2 days. (c) As in (a) but for named storms lasting >2 days. Dashed lines in each panel represent linear trends from 1990–2020.

Figure 3 displays global hurricane, major hurricane, and Category 4–5 hurricane numbers, as well as the percentage of hurricanes reaching Category 4–5 intensity from 1990–2020. Consistent with Fig. 1d, there has been a significant decreasing trend in global hurricane activity, with a significant decrease in western North Pacific hurricane activity being the primary driver (Fig. 3a). North Atlantic hurricane activity has increased by 0.7 hurricanes per decade, but this increase is not statistically significant. All other basins have exhibited relatively small insignificant trends.

While there has been a decreasing trend in hurricane activity, major hurricane and Category 4–5 hurricane activity has increased (although insignificantly) since 1990 (Fig. 1e, 1f, 3b, 3c). The overall increasing trend in Category 4–5 hurricanes accompanied by a decreasing trend in all hurricanes indicates a shift towards more intense global hurricane activity and a higher Category 4–5 percentage (Fig. 3d) as noted by Elsner et al. (2008) and Kossin et al. (2020).

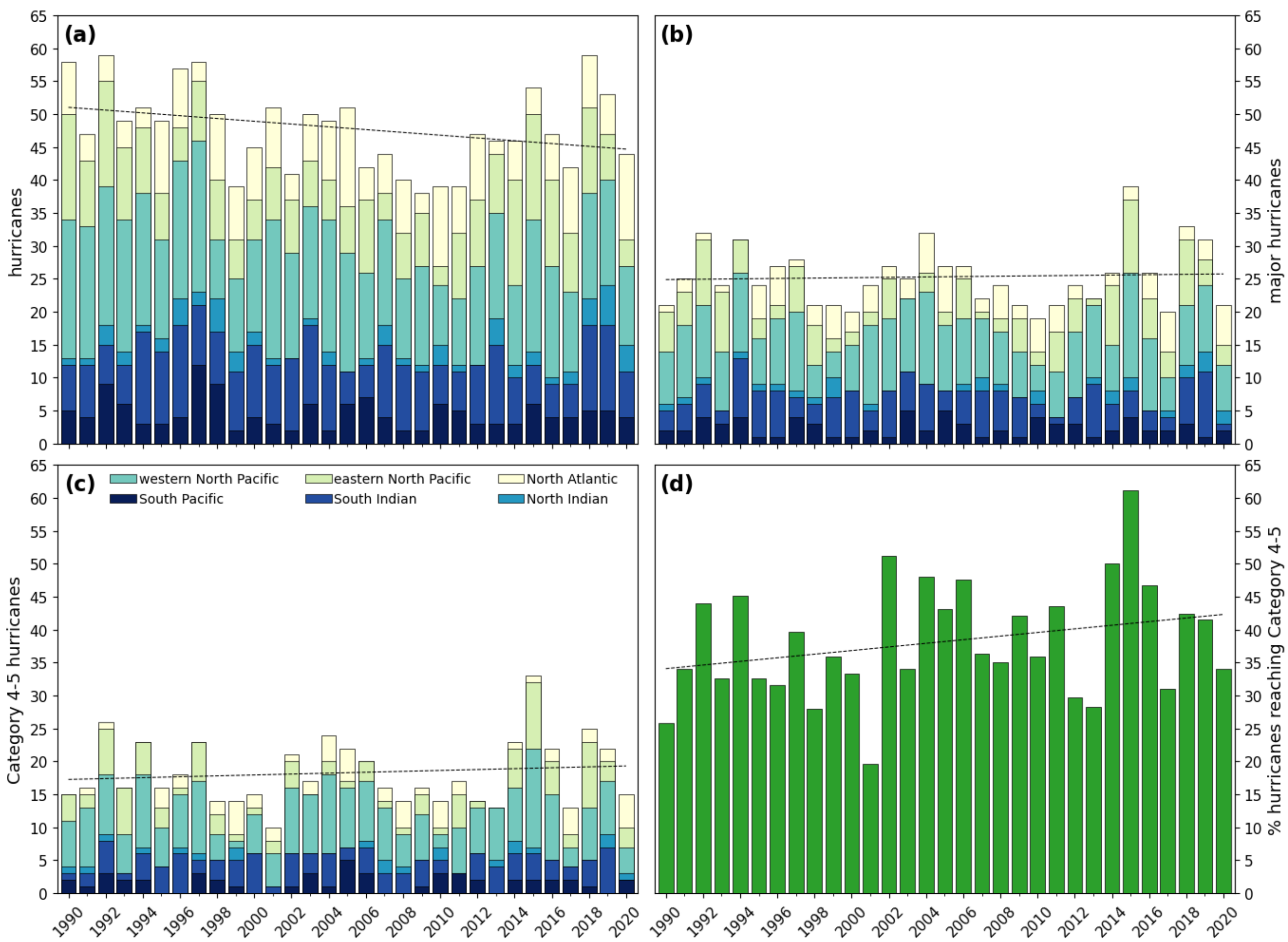

Figure 3. As in Figure 2 but for (a) hurricanes, (b) major hurricanes, and (c) Category 4–5 hurricanes. (d) Global percentage of hurricanes reaching Category 4–5 intensity.

Global ACE has significantly decreased since 1990 (Fig. 1h, 4a), indicating that global decreases in frequency and duration of TCs currently dominate over the increase in hurricane severity (Fig. 3d). As was the case with hurricane numbers, the western North Pacific has exhibited a significant decreasing trend in ACE since 1990, with ACE also decreasing significantly in the South Indian Ocean. The North Atlantic shows the largest overall increasing trend, although given large year-to-year volatility, this trend is not significant.

The 30 kt day^{-1} criterion has been frequently used to define RI in past studies (e.g., Kaplan & DeMaria, 2003; and many others), but this metric shows relatively small changes in most basins except the North Atlantic which shows a significant (at the 10% level) increasing trend (Table S2). Global trends are not statistically significant; however, the global trend in 24-h intensification periods for a higher RI threshold (50 kt day^{-1}) is significant at the 5% level (Fig. 1i, 4b), corroborating Bhatia et al. (2019). All six basins show an increasing trend in these events, with significant (at the 10% level) increasing trends in the western North Pacific, North Indian, and South Indian basins. The number of RW events at the -50 kt day^{-1} threshold is also trending upward, though the global total has not increased significantly (Fig. 1i, 4b). Global increases in -30 kt day^{-1} RW events are insignificant (Table S2).

Corroborating Weinkle et al. (2012), we find a significant increase in global damage (Fig. 1i, 4d) as well as significant increases in the western North Pacific, North Indian, and South Pacific basins. The linear trend in North Atlantic damage is sizable, but given the extremely large year-to-year volatility in damage and the use of least-squares linear trend analysis, the increase does not reach statistical significance. These increases in physical damage and/or direct loss costs are generally the result of increases in coastal population and the value of physical structures or non-physical risk exposure (Klotzbach et al., 2018; Weinkle et al., 2018). However, we note that a growing portion of observed damage may also reflect increases in storm severity (Grinsted et al., 2019) as well as increases in tertiary storm impacts such as greater rainfall and background sea level rise (Knutson et al., 2020). These storm impacts have highlighted the vulnerabilities of coastal exposures that require expenditures to modernize and/or retrofit local infrastructure and regional residential and commercial exposure, and the importance of updating and enforcing local building codes.

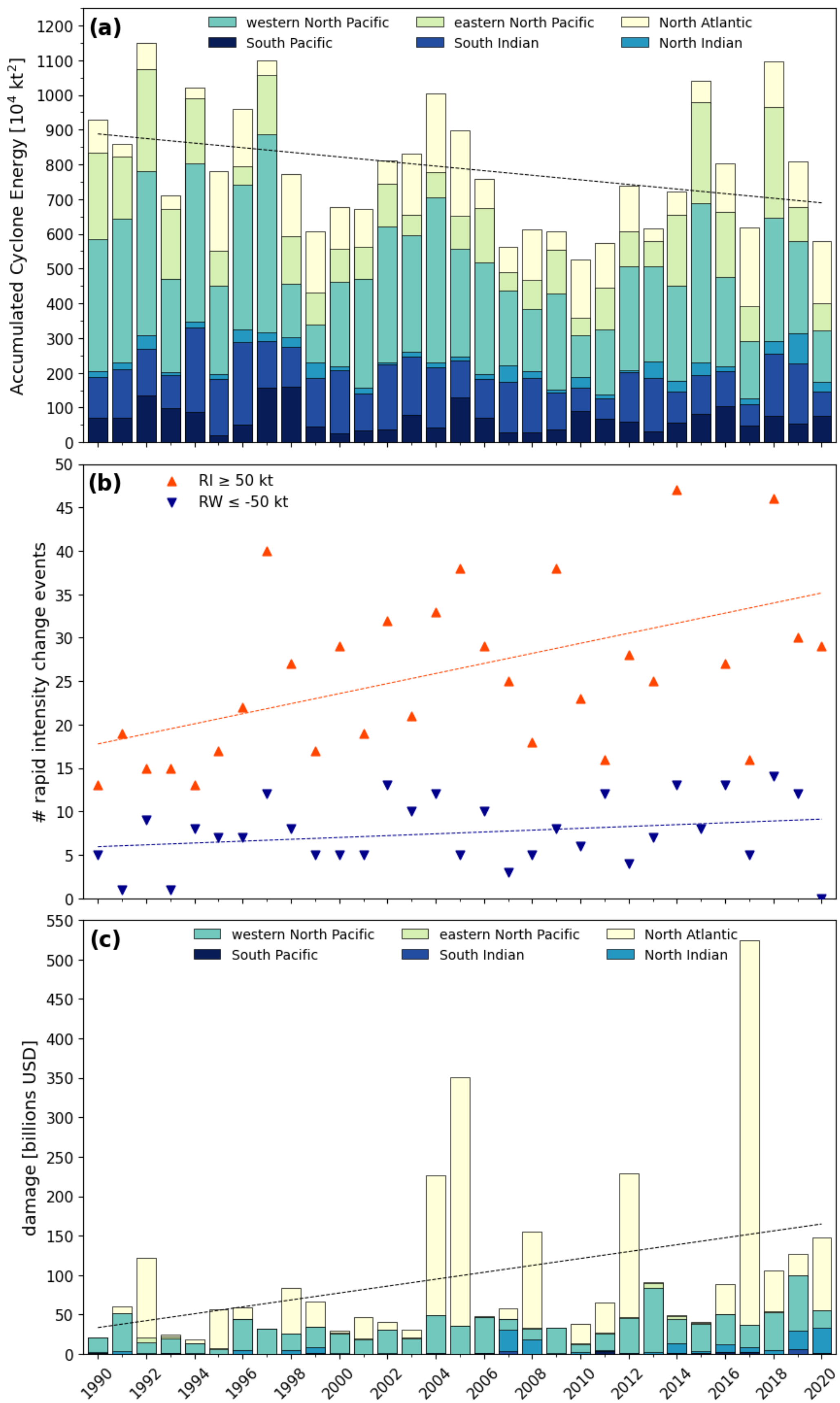
(a)
western North Pacific
eastern North Pacific
North Atlantic
South Pacific
South Indian
North Indian
Accumulated Cyclone Energy [10^4 kt^2]
(b)
RI ≥ 50 kt
RW ≤ -50 kt
rapid intensity change events
(c)
damage [billions USD]

Figure 4. (a) As in Figure 2 but for Accumulated Cyclone Energy (10^4 kt^2). (b) Global rapid intensity change events for the 50-kt RI and -50-kt RW thresholds. (c) As in Figure 1 but for damage (billions USD).

4 Large-Scale Drivers of Observed Trends

We now turn our attention to the large-scale atmospheric/oceanic drivers of these observed TC trends by exploring spatial patterns of 1990–2020 annually-averaged trends (Fig. 5). Some of the most notable TC signals in the past 30 years have been the significant decreasing trends in western North Pacific hurricane numbers and ACE, as well as the increasing trend in the percentage of Category 4–5 hurricanes and 50-kt RI storms. Increasing shear is seen across much of the central Pacific (Fig. 5a) though these trends are near zero in the most active regions of the northern hemisphere basins. Mid-level moisture has decreased over portions of the Pacific, but moisture increased over the Maritime Continent and parts of the Indian Ocean, with some regions achieving statistical significance (Fig. 5b). Notably, potential intensity (PI) has increased across most tropical basins (Fig. 5c) largely co-located with rising SSTs (Fig. 5d) that are statistically significant at the 5% level. The increasing SST and especially potential intensity may be responsible for the observed increase in 50-kt RI TC periods. We find similar patterns in maps of differences between the 2006-2020 and 1990-2005 averages (not shown).

Increasing upper-level temperatures help explain the more moderate trends in PI compared with SST (not shown). When examining annual averages computed within 30° longitude bins between 10-20°N and 10-20°S, 200-hPa temperature always exhibited a positive trend. These trends were statistically significant at the 5% level in all Northern Hemisphere bins and all Southern Hemisphere bins between 180° and 0°.

Finally we highlight trends in the ELI (Fig. 5e), as ENSO has been shown in prior studies to be a significant driver of TC activity in all oceanic basins (e.g., Camargo et al., 2007). From 1990–2020, there has been a statistically significant (at the 10% level) westward shift in the annually-averaged ELI, indicating a stronger and westward-shifted Walker Circulation, also recently noted by Seager et al. (2019) and Zhao and Allen (2019). This trend towards a more La Niña-like base state is consistent with the observed atmospheric/oceanic pattern changes as well as the decreasing trend in western North Pacific ACE and increasing trend in North Atlantic ACE that have been observed since 1990.

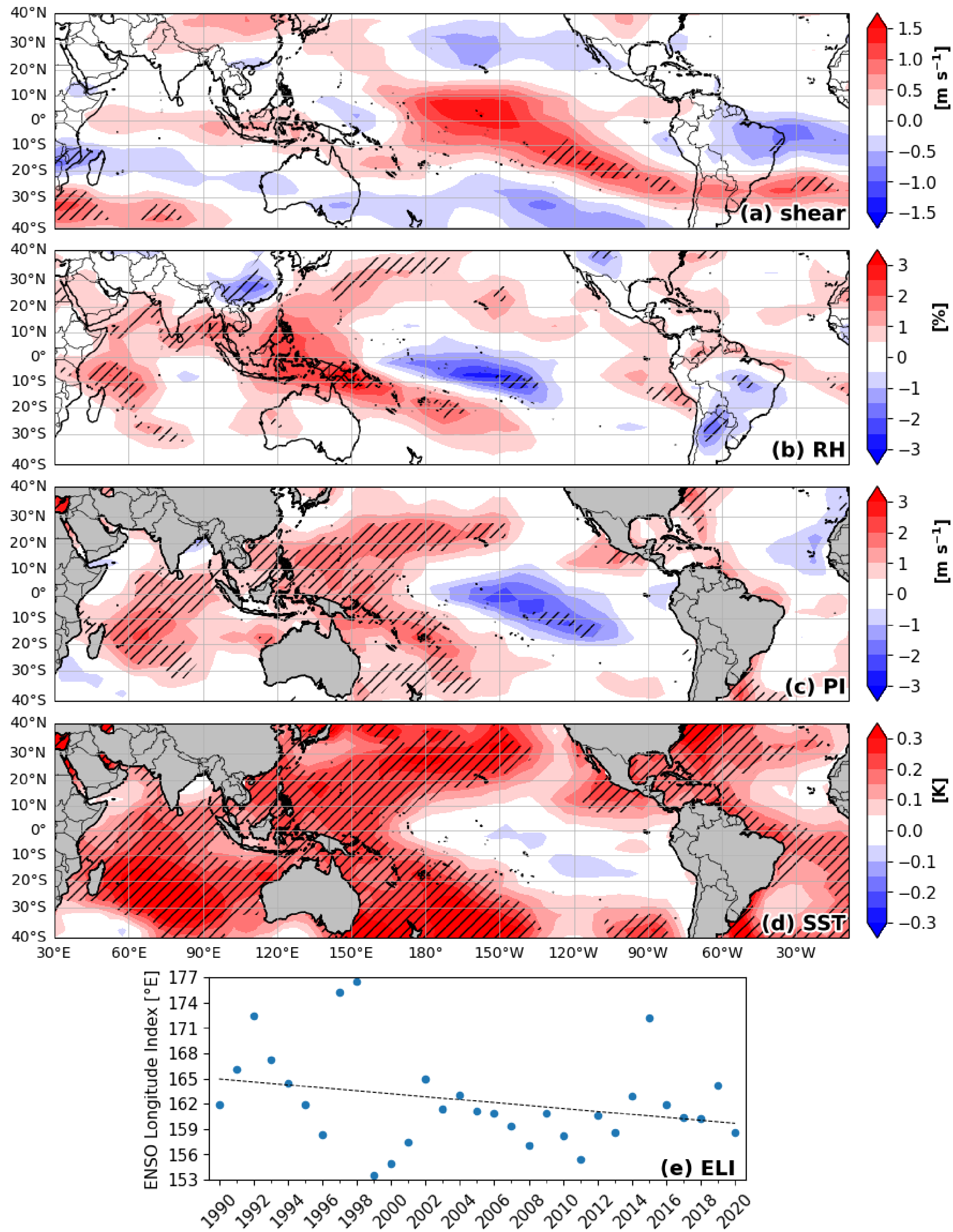

(a) shear
[m s^{-1}]
(b) RH
[%]
(c) PI
[m s^{-1}]
(d) SST
[K]
(e) ELI
ENSO Longitude Index [°E]

Figure 5. Maps of 1990–2020 per-decade trend values (shaded) and annual trend p-values <= 0.05 (hatching) for ERA5 annually-averaged (a) 200-850-hPa vertical wind shear [m s^{-1}], (b) 500-700-hPa relative humidity [%], (c) potential intensity [m s^{-1}], and (d) sea surface temperature [K]. ERA5 data averaged over 5° x 5° boxes prior to computing trends. Panel (e) shows annually-averaged ELI (°E, dots) and the 31-year trend (dashed line).

5 Conclusions

By investigating global TC activity from 1990–2020, we find significant decreasing trends in global hurricane numbers and ACE, primarily due to a significant decreasing trend in these metrics in the western North Pacific. This decreasing trend is likely linked to a trend towards a more La Niña-like base state. Short-lived named storms (<= 2 days) have increased globally, with most of this increase coming from the North Atlantic and eastern North Pacific basins. We also find significant global increases in 50+ kt day^{-1} RI storms and global damage / direct loss costs.

The increase in short-lived named storms is primarily due to improvements in observational technology, including microwave sensors and scatterometry (Landsea et al., 2010). The increase in high-end RI storms is likely due to higher SSTs and especially increased potential intensity (Fig. 4), while the increase in global damage is likely due to increases in population and wealth in coastal regions (Weinkle et al., 2012; Klotzbach et al., 2018).

Acknowledgments

P. Klotzbach would like to acknowledge a grant from the G. Unger Vetlesen Foundation. K. Wood acknowledges support from National Science Foundation award AGS-2011812 and Mississippi State University's Office of Research and Economic Development. C. Patricola acknowledges support from the U.S. Department of Energy, Office of Science, Office of Biological and Environmental Research, Earth and Environmental Systems Modeling Program, under Early Career Research Program Award Number DE-SC0021109. C. Schreck was supported by NOAA through the Cooperative Institute for Satellite Earth System Studies under Cooperative Agreement NA19NES4320002. M. Bell acknowledges support from Office of Naval Research award N000142012069.

Data Availability Statement

Tropical cyclone data were taken from the International Best Track Archive for Climate Stewardship version 4 (IBTrACS v4): https://www.ncdc.noaa.gov/ibtracs/index.php?name=ib-v4-access. All atmospheric and oceanic data were obtained from the European Centre for Medium Range Weather Forecasts Reanalysis 5 (ERA5): https://www.ecmwf.int/en/forecasts/datasets/reanalysis-datasets/era5. The ENSO Longitude

Index was taken from: https://portal.nersc.gov/archive/home/projects/cascade/www/ELI. EM-DAT is available at: https://public.emdat.be/.

References

Balagaru, K., Foltz, G. R., & Leung, L. R. (2018). Increasing magnitude of hurricane rapid intensification in the eastern and central tropical Atlantic. *Geophysical Research Letters*, 45(9), 4238–4247. https://doi.org/10.1029/2018GL077597

Barnston, A. G., Chelliah, M., & Goldenberg, S. B. (1997). Documentation of a highly ENSO-related SST region in the equatorial Pacific: Research note. *Atmosphere-Ocean,* 35(3), 367–383. https://doi.org/10.1080/07055900.1997.9649597

Bell, G. D., Halpert, M. S., Schnell, R. C., Higgins, R. W., Lawrimore, J., Kousky, V. E., Tinker, R., et al. (2000). Climate assessment for 1999. *Bulletin of the American Meteorological Society,* 81(6), S1–S50. https://doi.org/10.1175/1520-0477(2000)81[s1:CAF]2.0.CO;2

Bhatia, K. T., Vecchi, G. A., Knutson, T. R., Murakami, H., Kossin, J., Dixon, K. W., & Whitlock, C. E. (2019). Recent increases in tropical cyclone intensification rates. *Nature Communications*, 10(1), 1–9. https://doi.org/10.1038/s41467-019-08471-z

Camargo, S. J., Emanuel, K. A., & Sobel, A. H. (2007). Use of a genesis potential index to diagnose ENSO effects on tropical cyclone genesis. *Journal of Climate,* 20(19), 4819–4834, https://doi.org/10.1175/JCLI4282.1

Chu, J.-H., Sampson, C. R., Levine A. S., & Fukada, E. (2002). The Joint Typhoon Warning Center best-tracks, 1945–2000. Naval Research Laboratory Reference Number NRL/MR/7540-02-16. https://www.metoc.navy.mil/jtwc/products/best-tracks/tc-bt-report.html

Elsner, J. B., Kossin, J. P., & Jagger, T. H. (2008). The increasing intensity of the strongest tropical cyclones. *Nature,* 455, 92-95. https://doi.org/10.1038/nature07234

EM-DAT. The International Disaster Database. Accessed on 18 March 2021. https://public.emdat.be

Grinsted, A., Ditlevsen, P.,. & Christensen, J. H. (2019). Normalized US hurricane damage estimates using area of total destruction, 1900-2018. *Proceedings of the National Academy of Sciences*, 116(48), 23942-23946. https://doi.org/10.1073/pnas.1912277116

Hart, R. E. (2003). A cyclone phase space derived from thermal wind and thermal asymmetry. *Monthly Weather Review*, 131(4), 585-616. https://doi.org/10.1175/1520-0493(2003)131%3C0585:ACPSDF%3E2.0.CO;2

Hersbach, H., Bell, B., Berrisford, P., Hirahara, S., Horanyi, A., Munoz-Sabater, J., Nicolas, J., et al. (2020). The ERA5 global reanalysis. *Quarterly Journal of the Royal Meteorological Society,* 146(730), 1999-2049. https://doi.org/10.1002/qj.3803

Huang, B., Thorne, P. W., Banzon, V. F., Boyer, T., Chepurin, G., Lawrimore, J. H., Menne, M. J., et al. (2017). Extended Reconstructed Sea Surface Temperature version 5 (ERSSTv5), Upgrades, validations, and intercomparisons. *Journal of Climate,* 30(2), 8179-8205. https://doi.org/10.1175/JCLI-D-16-0836.1

Kaplan, J., & DeMaria, M. (2003). Large-scale characteristics of rapidly intensifying tropical cyclones in the North Atlantic basin, *Weather and Forecasting*, *18*(6), 1093-1108. https://doi.org/10.1175/1520-0434(2003)018%3C1093:LCORIT%3E2.0.CO;2

Klotzbach, P. J. (2006). Trends in global tropical cyclone activity over the past twenty years (1986-2005). *Geophysical Research Letters,* 33(10), L10805. https://doi.org/10.1029/2006GL025881

Klotzbach, P. J., Bowen, S. G., Pielke Jr., R., and Bell, M. M.. (2018). Continental United States landfall frequency and associated damage: Observations and future risks. *Bulletin of the American Meteorological Society,* 99(7), 1359–1376, https://doi.org/10.1175/BAMS-D-17-0184.1

Klotzbach, P. J., & Landsea, C. W. (2015). Extremely intense hurricanes: Revisiting Webster et al. (2005) after 10 years. *Journal of Climate,* 28(19), 7621–7629. https://doi.org/10.1175/JCLI-D-15-0188.1

Knapp, K. R., & Kossin, J. P. (2007). New global tropical cyclone data set from ISCCP B1 geostationary satellite observations. *Journal of Applied Remote Sensing,* 1(1), 013505. https://doi.org/10.1117/1.2712816

Knapp, K. R., Kruk, M. C., Levinson, D. H., Diamond, H. J., & Neumann, C. J. (2010). The International Best Track Archive for Climate Stewardship (IBTrACS): Unifying tropical cyclone data. *Bulletin of the American Meteorological Society*, 91(3), 363–376. https://doi.org/10.1175/2009BAMS2755.1

Knutson, T., Camargo, S. J., Chan, J. C. L., Emanuel, K., Ho, C., Kossin, J., Mohapatra, M., et al. (2019). Tropical cyclones and climate change assessment: Part I: Detection and attribution, *Bulletin of the American Meteorological Society*, *100*(10), 1987–2007, https://doi.org/10.1175/BAMS-D-18-0189.1

Knutson, T., Camargo, S. J., Chan, J. C. L., Emanuel, K., Ho, C., Kossin, J., Mohapatra, M., et al. (2020). Tropical cyclones and climate change assessment: Part II: Projected response to anthropogenic warming, *Bulletin of the American Meteorological Society*, *100*(10), E303–322, https://doi.org/10.1175/BAMS-D-18-0194.1

Kossin, J. P., Knapp, K. R., Olander, T. L., & Velden, C. S. (2020). Global increases in major tropical cyclone exceedance probability over the past four decades. *Proceedings of the National Academy of Sciences,* 117(22), 11975–11980. https://doi.org/10.1073/pnas.1920849117

Landsea, C. W., & Franklin, J. L. (2013). Atlantic hurricane database uncertainty and presentation of a new database format. *Monthly Weather Review*, 141(10), 3576–3592. https://doi.org/10.1175/MWR-D-12-00254.1

Landsea, C. W., Harper, B. A., Hoarau, K., & Knaff, J. A. (2006). Can we detect trends in extreme tropical cyclones? *Science,* 313, 452–454. https://doi.org/10.1126/science.1128448

Landsea, C. W., Vecchi, G. A., Bengtsson, L., & Knutson, T. R. (2010). Impact of duration thresholds on Atlantic tropical cyclone counts, *Journal of Climate*, 23(10), 2508-2519. https://doi.org/10.1175/2009JCLI3034.1

Mantua, N. J., & Hare, S. J. (2002). The Pacific Decadal Oscillation. *Journal of Oceanography,* 58(1), 35-44. https://doi.org/10.1023/A:1015820616384

Maue, R. N. (2011). Recent historically low global tropical cyclone activity, *Geophysical Research Letters,* 38, L14803, https://doi.org/10.1029/2011GL047711

Mendelsohn, R., Emanuel, K., Chonabayashi S., & Bakkensen L. (2012). The impact of climate change on global tropical cyclone damage. *Nature Climate Change*, 2, 205–209, https://doi.org/10.1038/nclimate1357.

Schreck, C. J., III, Knapp, K. R., & Kossin, J. P. (2014). The impact of best track discrepancies on global tropical cyclone climatologies using IBTrACS. *Monthly Weather Review*, 142(10), 3881-3899. https://doi.org/10.1175/MWR-D-14-00021.1

Seager, R., Cane, M., Henderson, N., Lee, D.-E., Abernathey, R., & Zhang, H. (2019). Strengthening tropical Pacific zonal sea surface temperature gradient consistent with rising greenhouse gases. *Nature Climate Change,* 9, 517-522, htttps://doi.org/10.1038/s41558-019-0505-x

Webster, P. J., Holland, G. J., Curry, J. A., & Chang, H.-R. (2005). Changes in tropical cyclone number, duration and intensity in a warming environment. *Nature,* 309(5742), 1844-1846, https://doi.org/10.1126/science.1116448

Weinkle, J., Maue, R., & Pielke Jr., R. P. (2012). Historical global tropical cyclone landfalls. *Journal of Climate,* 25(13)**,** 4729–4735. https://doi.org/10.1175/JCLI-D-11-00719.1

Weinkle, J., Landsea, C., Collins, D., Masulin, R., Crompton, R. P., Klotzbach, P. J., & Pielke Jr., R. P. (2018). Normalized hurricane damage in the continental United States 1900–2017. *Nature Sustainability,* 1(12)**,** 808–813. https://doi.org/10.1038/s41893-018-0165-2

Williams, I. N., & Patricola, C. M. (2018). Diversity of ENSO events unified by convective threshold sea surface temperature: A nonlinear ENSO index. *Geophysical Research Letters*, 45, 9236–9244. https://doi.org/10.1029/2018GL079203

Wood, K. M., & Ritchie, E. A. (2015). A definition for rapid weakening in the North Atlantic and eastern North Pacific. *Geophysical Research Letters*, 42, 10091–10097. https://doi.org/10.1002/2015GL066697

Zhao, X., & Allen, R. J. (2019). Strengthening of the Walker Circulation in recent decades and the role of natural sea surface temperature variability. *Environmental Research Communications,* 1(2), 021003. https://doi.org/10.1088/2515-7620/ab0dab

Geophysical Research Letters

Supporting Information for

Trends in Global Tropical Cyclone Activity: 1990-2020

P. J. Klotzbach[1], K. M. Wood[2*], C. J. Schreck[3], S. G. Bowen[4], C. M. Patricola[5], and M. M. Bell[1]

[1]Department of Atmospheric Science, Colorado State University, Fort Collins, CO, USA.

[2]Department of Geosciences, Mississippi State University, Mississippi State, MS, USA.

[3]Cooperative Institute for Satellite Earth System Studies (CISESS), North Carolina State University, Asheville, NC, USA.

[4]Aon, Chicago, IL, USA.

[5]Department of Geological and Atmospheric Sciences, Iowa State University, Ames, IA, USA.

*Klotzbach and Wood contributed equally to this work

Contents of this file

Introduction

This supporting information includes one additional figure and two additional tables. Figure S1 displays global rapid intensity change events at a 30-kt threshold from 1990-2020. Table S1 displays average values of various TC indices from 1990-2020. Table S2 displays linear per-decade trends in these TC indices from 1990-2020.

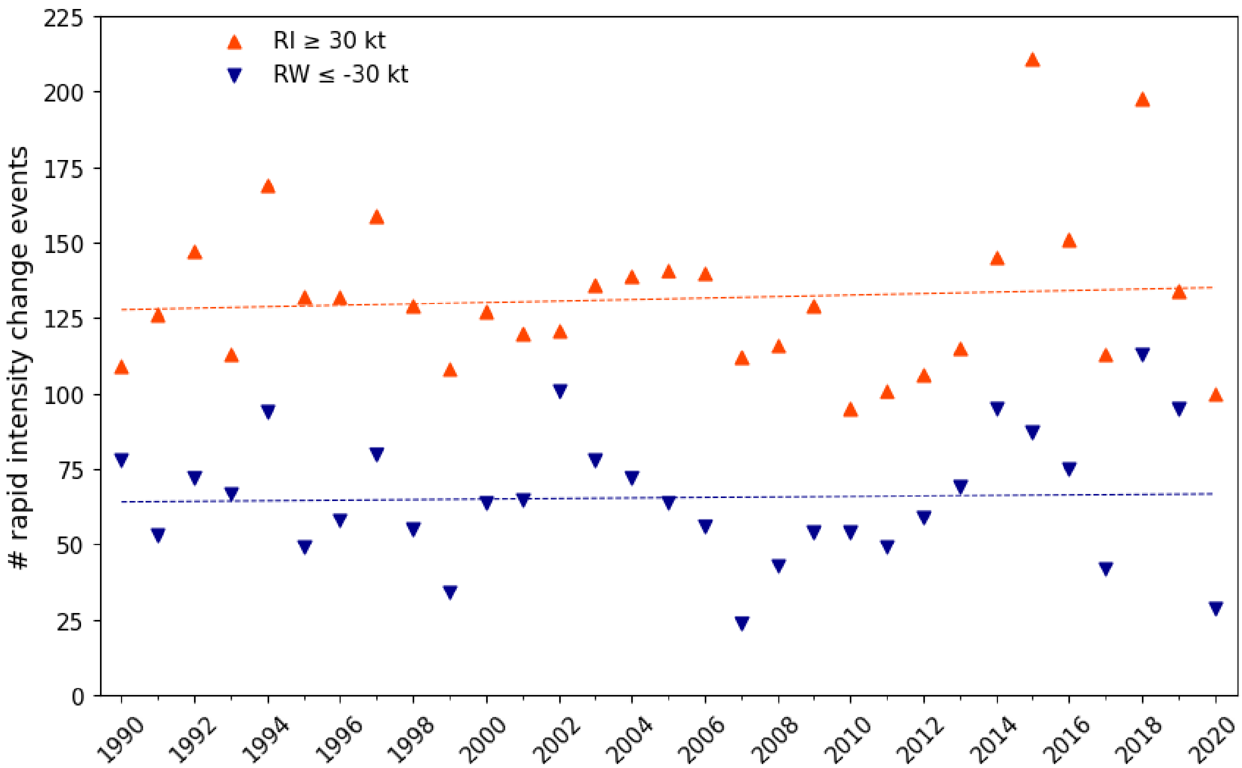

Figure S1. Global rapid intensity change events for the 30-kt RI and -30-kt RW thresholds.

Table S1. Average annual values for several TC metrics globally and for six individual TC basins during 1990-2020. The percentage of global TC activity generated in each basin is listed in parentheses.

TC Metric	Globe	North Atlantic	Eastern North Pacific	Western North Pacific	North Indian	South Indian	South Pacific
Named Storms	87.1	14.4 (17%)	16.7 (19%)	25.6 (29%)	5.2 (6%)	15.8 (18%)	9.3 (11%)
Named Storms <=2 Days	21.0	3.8 (18%)	4.2 (20%)	4.9 (23%)	2.1 (10%)	3.4 (16%)	2.7 (13%)
Named Storms >2 Days	66.0	10.6 (16%)	12.6 (19%)	20.7 (31%)	3.1 (5%)	12.4 (19%)	6.6 (10%)
Named Storm Days	409.9	69.4 (17%)	74.5 (18%)	134.4 (33%)	16.5 (4%)	76.3 (18%)	38.6 (11%)
Hurricanes	47.9	7.2 (15%)	9.1 (19%)	16.1 (34%)	2.1 (4%)	8.8 (18%)	4.6 (10%)
Hurricane Days	169.6	27.0 (15%)	29.4 (19%)	65.6 (34%)	4.3 (3%)	28.6 (17%)	14.7 (9%)
Major Hurricanes	25.3	3.1 (12%)	4.7 (18%)	9.2 (36%)	1.0 (4%)	4.9 (19%)	2.4 (10%)
Major Hurricane Days	58.0	7.2 (12%)	9.8 (17%)	24.9 (43%)	1.5 (3%)	9.8 (17%)	4.8 (8%)
Cat. 4–5 Hurricanes	18.3	1.9 (11%)	3.3 (18%)	7.5 (41%)	0.7 (4%)	3.3 (18%)	1.6 (9%)
Cat. 4–5 Hurricane %	38%	27%	37%	47%	32%	37%	34%
Cat. 4–5 Days	32.3	3.9 (12%)	4.7 (15%)	15.7 (49%)	0.8 (3%)	4.8 (15%)	2.4 (7%)
ACE (10^4 kt^2)	789	122 (15%)	137 (17%)	302 (38%)	24 (3%)	135 (17%)	70 (9%)
30-kt RI Events	131.4	15.9 (12%)	24.9 (19%)	48.6 (37%)	4.7 (4%)	24.3 (18%)	13.1 (10%)
50-kt RI Events	26.5	2.4 (9%)	5.5 (21%)	10.1 (38%)	1.0 (4%)	4.9 (18%)	2.6 (10%)
30-kt RW Events	65.4	3.7 (6%)	19.5 (30%)	16.6 (25%)	0.9 (1%)	16.9 (26%)	7.8 (12%)
50-kt RW Events	7.5	0.3 (4%)	2.0 (27%)	1.8 (24%)	0.1 (1%)	2.3 (31%)	1.1 (15%)
Damage (Billions USD)	99.3	61.2 (62%)	1.0 (1%)	30.4 (31%)	5.4 (5%)	0.4 (<1%)	0.7 (1%)

Table S2. As in Table S1 but for per-decade linear trends. Category 4-5 hurricane percentage linear trends are not displayed for the North Indian Ocean due to limited per-year hurricane formations. Trends significant at the 5% level are highlighted in bold-face, while trends significant at the 10% level are italicized.

TC Metric	Globe	North Atlantic	Eastern North Pacific	Western North Pacific	North Indian	South Indian	South Pacific
Named Storms	1.0	**2.7**	1.1	**-1.8**	0.3	-0.8	-0.5
Named Storms <=2 Days	**3.0**	**1.0**	**1.3**	0.4	0.1	-0.2	0.4
Named Storms >2 Days	-2.0	**1.8**	-0.2	**-2.3**	0.2	-0.6	-1.0
Named Storm Days	*-27.3*	9.2	-1.2	**-22.2**	1.4	**-9.4**	-5.0
Hurricanes	*-2.1*	0.7	-0.2	**-2.0**	0.4	-0.3	-0.5
Hurricane Days	**-20.3**	0.7	-3.5	**-12.6**	**1.5**	*-4.4*	-2.1
Major Hurricanes	0.3	0.5	0.0	-0.2	0.3	-0.2	-0.1
Major Hurricane Days	-4.8	1.2	-1.1	-3.9	0.5	-1.0	-0.4
Cat. 4–5 Hurricanes	0.7	0.5	0.2	-0.1	0.1	0.0	0.0
Cat. 4–5 Hurricane %	3%	5%	3%	4%	---	2%	4%
Cat. 4–5 Days	-2.5	0.7	-0.7	-2.2	0.3	-0.6	0.0
ACE	*-66*	14	-10	**-50**	5	*-18*	-8
30-kt RI Events	2.5	*4.0*	0.8	-1.8	0.8	-0.8	-0.5
50-kt RI Events	**5.8**	0.6	0.9	*2.1*	**0.7**	*1.4*	0.1
30-kt RW Events	0.9	0.8	0.0	-1.1	**1.1**	0.4	-0.4
50-kt RW Events	1.1	0.1	0.3	-0.2	0.2	*0.9*	-0.2
Damage (Billions USD)	**43.7**	31.0	0.0	**7.5**	**4.5**	0.4	**0.4**